Analytical solutions for free and forced vibrations of a multiple cracked Timoshenko beam subject to a concentrated moving load

Article *in* Acta Mechanica · September 2011

DOI: 10.1007/s00707-011-0495-x

CITATIONS
33

READS
862

2 authors:

Masoud Shafiei
Tarbiat Modares University
4 PUBLICATIONS **105** CITATIONS

SEE PROFILE

N. Khaji
Tarbiat Modares University
79 PUBLICATIONS **977** CITATIONS

SEE PROFILE

Acta Mech
DOI 10.1007/s00707-011-0495-x

M. Shafiei · N. Khaji

Analytical solutions for free and forced vibrations of a multiple cracked Timoshenko beam subject to a concentrated moving load

Received: 7 December 2010

Abstract An analytical approach for evaluating the forced vibration response of uniform beams with an arbitrary number of open edge cracks excited by a concentrated moving load is developed in this research. For this purpose, the cracked beam is modeled using beam segments connected by rotational massless linear elastic springs with sectional flexibility, and each segment of the continuous beam is assumed to satisfy Timoshenko beam theory. In this method, the equivalent spring stiffness does not depend on the frequency of vibration and is obtained from fracture mechanics. Considering suitable compatibility requirements at cracked sections and corresponding boundary conditions, characteristic equations of free vibration response are derived. Then, forced vibration response is treated under a moving load with a constant velocity. Using the determined eigenfunctions, the forced vibration response may be obtained by the modal superposition method. Finally, some parametric studies are presented to show the effects of crack parameters and moving load velocity.

1 Introduction

One of the key issues of evaluation of the structural systems is evaluating the response of the structures under service loads. Some structures such as bridges may experience fatigue phenomena or overloading, which may result in some cracks in these structures. These cracks may cause changes in the structural parameters (e.g., the stiffness of a structural member such as beam elements), which can change the dynamic properties (such as natural frequencies and mode shapes) [1,2]. Obviously, the response of structures under dynamic loads depends on the mentioned structural parameters. Consequently, cracks may significantly affect the behavior of these structures. Various analytical methods have been used to illustrate the dynamic behavior of damaged beams among which various approaches were employed to model the cracks in beams. One method models the crack by reducing the suitable section modulus [3], while another method tries to evaluate a local flexibility for the cracked section [4]. Neglecting the shear effects in bending, some models have been proposed, in which the cracked sections are replaced by a rotational massless spring [5–7]. Using the theory of fracture mechanics to describe the local flexibility of cracked section, the complete vibration behavior of a cracked Euler–Bernoulli beam faced with open cracks was developed [8]. In order to solve the crack problem, another class of crack detection approaches using numerical methods (e.g., finite element methods) was proposed [9–11].

The cracked beam problem usually consists of two main approaches. One approach tries to deal with the crack detection problem using direct and inverse solutions [4,12–14], while some other researchers are eager to understand the effects of the crack(s) on the response of the beam under various loading cases.

M. Shafiei · N. Khaji (✉)
Faculty of Civil and Environmental Engineering, Tarbiat Modares University,
P.O. Box 14115–397, Tehran, Iran
E-mail: nkhaji@modares.ac.ir
Tel.: +98-21-82883319
Fax: +98-21-82883381

Published online: 04 May 2011

The moving load problem represents a critical aspect in engineering [15,16]. Solving the moving load problem may help engineers to design the bridges and vehicles more efficiently. However, there are a few research works on the influence of the crack(s) on the response of beams under a moving load. Lee and Ng [17] analyzed the dynamic response of a simply supported beam with a single-sided crack subject to a moving force with constant velocity. Using the equivalent static load, Mahmoud [18] determined the stress intensity factor for a crack in a cracked beam under the moving force. Lin and Chang obtained the response of a cracked beam under the moving load using the modal expansion method [19]. In some research works, cracked beams with FGM materials under a moving load are investigated (see for example [20]).

All above studies on the moving load problem of cracked beams are based on the Euler–Bernoulli beam theory, in which the effect of shear deformations has been neglected.

In this study, attention is devoted to propose analytical expressions for evaluating eigenfunctions of multiple cracked Timoshenko cantilever beams. The present method is according to modeling the multiple cracked beams as segments connected by elastic massless rotational springs illustrating open-cracked cross-sectional flexibilities. Afterward, differential equations for free vibrations are established for each segment. For solving the differential equations, the characteristic equation of the problem is then expressed as a fourth-order determinant, equated to zero. As a result, the eigenfrequencies and eigenfunctions of the problem may be explicitly derived. The forced vibration response of the problem is then treated under a moving load with a constant velocity. For this purpose, the modal superposition method using the determined eigenfunctions is employed. In addition, various parametric studies are performed to illustrate the effects of crack parameters and moving load velocity.

2 Free vibration

We consider an elastic sound/uncracked Timoshenko beam of length L, with uniform cross-section A, moment of inertia I, and specified boundary conditions (B.C.) at the left and right ends of the beam. Using Hamilton's principle, one may readily derive the coupled Euler–Lagrange equations of the free bending vibrations of this beam [21] in the following form:

$$k'G\left(\frac{\partial^2 y(x,t)}{\partial x^2}-\frac{\partial \psi(x,t)}{\partial x}\right)-\rho\frac{\partial^2 y(x,t)}{\partial t^2}=0 \tag{1.1}$$

and

$$EI\frac{\partial^2 \psi(x,t)}{\partial x^2}+k'GA\left(\frac{\partial y(x,t)}{\partial x}-\psi(x,t)\right)-\rho I\frac{\partial^2 \psi(x,t)}{\partial t^2}=0, \tag{1.2}$$

where $y(x,t)$ is the transverse deflection function, and $\psi(x,t)$ is the slope of the deflection curve due to bending. Parameters E, G, and ρ represent Young's modulus, the shear modulus, and the material mass density, respectively. k' indicates the Timoshenko shear coefficient introduced to account for the geometry-dependent distribution of shear stress. One may rewrite Eqs. (1.1) and (1.2) in terms of the transverse deflection $y(x,t)$ alone by eliminating $\psi(x,t)$ from these equations. This yields to the single Timoshenko beam equation of free vibration as below,

$$EI\frac{\partial^4 y(x,t)}{\partial x^4}+\rho A\frac{\partial^2 y(x,t)}{\partial t^2}-\rho I\left(1+\frac{E}{k'G}\right)\frac{\partial^4 y(x,t)}{\partial t^2\partial x^2}+\frac{\rho^2 I}{k'G}\frac{\partial^4 y(x,t)}{\partial t^4}=0. \tag{2.1}$$

In a similar manner, Eqs. (1.1) and (1.2) can be written in terms of the deflection slope alone as

$$EI\frac{\partial^4 \psi(x,t)}{\partial x^4}+\rho A\frac{\partial^2 \psi(x,t)}{\partial t^2}-\rho I\left(1+\frac{E}{k'G}\right)\frac{\partial^4 \psi(x,t)}{\partial t^2\partial x^2}+\frac{\rho^2 I}{k'G}\frac{\partial^4 \psi(x,t)}{\partial t^4}=0. \tag{2.2}$$

The solution of the partial differential Eqs. (2.1) and (2.2) is found by using the separation of variables method in the following forms:

$$y(x,t)=LU(x)\exp(\mathrm{j}\omega t) \tag{3.1}$$

and

$$\psi(x,t)=\Psi(x)\exp(\mathrm{j}\omega t), \tag{3.2}$$

where $\mathrm{j} = \sqrt{-1}$, ω represents the frequency of vibrations, and $U(x)$and $\Psi(x)$ denote the normal function of $y(x,t)$and $\psi(x,t)$, respectively.

By substituting Eqs. (3.1) and (3.2) into Eqs. (2.1) and (2.2) and using the following new variables and constants:

$$\xi = \frac{x}{L}, \quad \varsigma = \frac{t}{\sqrt{L}}, \quad \vartheta = \frac{E}{k'G}, \quad r = \frac{I}{AL^2}, \quad s = \vartheta r, \quad \alpha = \frac{\rho A}{EI}L^4\omega^2, \tag{4}$$

one may easily derive the below expressions:

$$U^{iv}(\xi) + \alpha(r+s)U''(\xi) + \alpha(\alpha rs - 1)U(\xi) = 0 \tag{5.1}$$

and

$$\Psi^{iv}(\xi) + \alpha(r+s)\Psi''(\xi) + \alpha(\alpha rs - 1)\Psi(\xi) = 0. \tag{5.2}$$

The above equations should be solved with specified boundary conditions. Let us define the following parameters:

$$a = \frac{\alpha(r+s)}{2}, \quad b = \alpha(\alpha rs - 1), \quad \beta_1 = \sqrt{\sqrt{a^2 - b} - a}, \quad \beta_2 = \sqrt{\sqrt{a^2 - b} + a} \tag{6.1}$$

and

$$m_1 = \frac{\alpha s + \beta_1^2}{\beta_1}, \quad m_2 = \frac{\alpha s - \beta_2^2}{\beta_2}, \tag{6.2}$$

then the general solution of Eqs. (5.1) and (5.2) may be derived, for example in [22], in the following form:

$$U(\xi) = A\cosh\beta_1\xi + B\sinh\beta_1\xi + C\cos\beta_2\xi + D\sin\beta_2\xi \tag{7.1}$$

and

$$\Psi(\xi) = Am_1\sinh\beta_1\xi + Bm_1\cosh\beta_1\xi + Cm_2\sin\beta_2\xi - Dm_2\cos\beta_2\xi, \tag{7.2}$$

in which A, B, C and D are unknown constants.

Now, we consider a Timoshenko beam with an arbitrary number of single- or double-sided open cracks as shown in Fig. 1. The length of the beam is L, and the crack positions are at $\xi_i = e_i$. In order to solve the free vibration problem of the beam, the entire beam is now divided into m beam segments, and the crack positions are assumed as the separation points. The beam segments may be treated separately. It is assumed that cracks remain open during the beam vibration. Moreover, we assume that the entire beam has a uniform cross-section except at the crack locations. The equations of motion for these segments may be given as

$$U_i^{iv}(\xi) + \alpha(r+s)U_i''(\xi) + \alpha(\alpha rs - 1)U_i(\xi) = 0, \quad e_{i-1} < \xi < e_i \tag{8.1}$$

and

$$\Psi_i^{iv}(\xi) + \alpha(r+s)\Psi_i''(\xi) + \alpha(\alpha rs - 1)\Psi_i(\xi) = 0, \quad e_{i-1} < \xi < e_i, \tag{8.2}$$

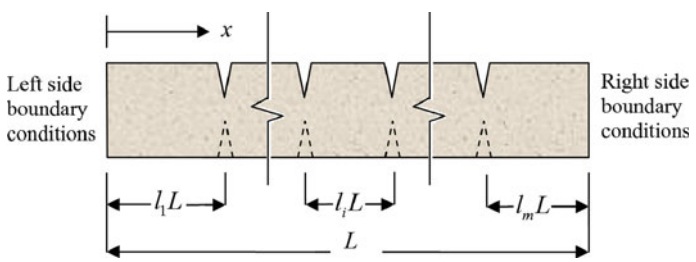

Fig. 1 Timoshenko beam with arbitrary number of single-sided (*filled*)—or double-sided (*filled and dashed*) open cracks

where $U_i(\xi)$ and $\Psi_i(\xi)$ denote the transverse deflection function and the slope function of each segment, respectively ($i = 1, 2, \ldots, m$). The general solution of Eqs. (8.1) and (8.2) for each segment may be written as

$$\begin{aligned} U_i(\xi - e_{i-1}) = A_i \cosh \beta_1(\xi - e_{i-1}) + B_i \sinh \beta_1(\xi - e_{i-1}) \\ + C_i \cos \beta_2(\xi - e_{i-1}) + D_i \sin \beta_2(\xi - e_{i-1}) \end{aligned} \tag{9.1}$$

and

$$\begin{aligned} \Psi_i(\xi - e_{i-1}) = A_i m_1 \sinh \beta_1(\xi - e_{i-1}) + B_i m_1 \cosh \beta_1(\xi - e_{i-1}) \\ + C_i m_2 \sin \beta_2(\xi - e_{i-1}) - D_i m_2 \cos \beta_2(\xi - e_{i-1}), \end{aligned} \tag{9.2}$$

in which A_i, B_i, C_i, and D_i are unknown constants related to the i-th segment.

The conditions for continuity of displacement, moment, and shear force at the crack locations are written in the following form, respectively:

$$U_{i+1}|_{\xi=e_i} = U_i|_{\xi=e_i}, \tag{10.1}$$

$$\Psi'_{i+1}\big|_{\xi=e_i} = \Psi'_i\big|_{\xi=e_i}, \tag{10.2}$$

$$(U'_{i+1} - \Psi_{i+1})\big|_{\xi=e_i} = (U'_i - \Psi_i)\big|_{\xi=e_i}. \tag{10.3}$$

Moreover, to consider the crack effects, the cracked section can be modeled as a local flexibility, which may principally be assumed as a rotational massless spring. The discontinuity in the slope of the beam at the cracked section may be implemented as the following relation (see for example [23]):

$$(U'_{i+1} - U'_i)\big|_{\xi=e_i} = \theta_i \Psi'_{i+1}\big|_{\xi=e_i}, \tag{10.4}$$

in which θ_i denotes the non-dimensional crack sectional flexibility, which depends on the crack extension. This function for a single-sided open crack is given [24] as

$$\theta_i = 6\pi \frac{H}{L} \eta_i^2 f_J(\eta_i), \tag{11.1}$$

in which η_i represents a non-dimensional crack depth ratio as

$$\eta_i = \frac{a_i}{H}, \tag{11.2}$$

where a_i is the crack depth, H is the beam depth, and

$$\begin{aligned} f_J(\eta_i) = 0.6384 - 1.035\eta_i + 3.7201\eta_i^2 - 5.1773\eta_i^3 \\ + 7.553\eta_i^4 - 7.332\eta_i^5 + 2.4909\eta_i^6. \end{aligned} \tag{11.3}$$

Similar equations are available in [24] for a double-sided open crack.

Employing Eqs. (10.1)–(10.4), the constants in the $(i+1)$-th segment of the beam (A_{i+1}, B_{i+1}, C_{i+1}, and D_{i+1}) with the length of l_{i+1} are related to those in the i-th segment (A_i, B_i, C_i, and D_i) with the length of l_i, in a form of a simultaneous system of equations as

$$\{\mathrm{A}\}_{(i+1)} = [\mathrm{Z}]_{(i)} \{\mathrm{A}\}_{(i)}, \tag{12}$$

where $\{\mathrm{A}\}_{(i)}$ and $\{\mathrm{A}\}_{(i+1)}$ indicate the unknown constants vectors of the i-th and the $(i+1)$-th segments of the beam, respectively; $[\mathrm{Z}]_{(i)}$ represents a transformation/mapping matrix being a function of θ_i and ω.

After some algebraic manipulations, the components z_{ij} of 4×4 mapping matrix $[Z]_{(i)}$ may be obtained as the following expressions:

$$z_{11} = \cosh \beta_1 l_i, \quad z_{12} = \sinh \beta_1 l_i, \quad z_{13} = 0, \quad z_{14} = 0, \tag{13.1}$$

$$z_{21} = \frac{\beta_2 m_2}{\beta_2 m_1 + \beta_1 m_2} \left(\frac{\beta_1}{\beta_2} m_1 \theta_i \cosh \beta_1 l_i + \frac{\beta_1}{\beta_2} \sinh \beta_1 l_i + \frac{m_1}{m_2} \beta_1 \theta_i \cosh \beta_1 l_i + \frac{m_1}{m_2} \sinh \beta_1 l_i \right), \tag{13.2}$$

$$z_{22} = \frac{\beta_2 m_2}{\beta_2 m_1 + \beta_1 m_2} \left(\frac{\beta_1}{\beta_2} m_1 \theta_i \sinh \beta_1 l_i + \frac{\beta_1}{\beta_2} \cosh \beta_1 l_i + \frac{m_1}{m_2} \beta_1 \theta_i \sinh \beta_1 l_i + \frac{m_1}{m_2} \cosh \beta_1 l_i \right), \tag{13.3}$$

$$z_{23} = \frac{\beta_2 m_2}{\beta_2 m_1 + \beta_1 m_2} \theta_i (m_2 + \beta_2) \cos \beta_2 l_i, \quad z_{24} = \frac{\beta_2 m_2}{\beta_2 m_1 + \beta_1 m_2} \theta_i (m_2 + \beta_2) \sin \beta_2 l_i, \tag{13.4}$$

$$z_{31} = 0, \quad z_{32} = 0, \quad z_{33} = \cos \beta_2 l_i, \quad z_{34} = \sin \beta_2 l_i, \tag{13.5}$$

$$z_{41} = \frac{\beta_1 m_1}{\beta_2 m_1 + \beta_1 m_2} \theta_i (m_1 - \beta_1) \cosh \beta_1 l_i, \quad z_{42} = \frac{\beta_1 m_1}{\beta_2 m_1 + \beta_1 m_2} \theta_i (m_1 - \beta_1) \sinh \beta_1 l_i, \tag{13.6}$$

$$z_{43} = \frac{\beta_1 m_1}{\beta_2 m_1 + \beta_1 m_2} \left(\frac{\beta_2}{\beta_1} m_2 \theta_i \cos \beta_2 l_i - \frac{\beta_2}{\beta_1} \sin \beta_2 l_i - \frac{m_2}{m_1} \beta_2 \theta_i \cos \beta_2 l_i - \frac{m_2}{m_1} \sin \beta_2 l_i \right), \tag{13.7}$$

$$z_{44} = \frac{\beta_1 m_1}{\beta_2 m_1 + \beta_1 m_2} \left(\frac{\beta_2}{\beta_1} m_2 \theta_i \sin \beta_2 l_i + \frac{\beta_2}{\beta_1} \cos \beta_2 l_i - \frac{m_2}{m_1} \beta_2 \theta_i \sin \beta_2 l_i + \frac{m_2}{m_1} \cos \beta_2 l_i \right). \tag{13.8}$$

Consequently, in each crack position, the four constants in the right side of the crack can be mapped into those of the left side, which leads to reducing the number of independent constant into four ones. These remaining constants may be found by applying the boundary conditions at the two ends of the entire Timoshenko beam. The effects of various types of boundary conditions may be taken into account in the final step of the solution. In this Section, a cantilever beam is considered to be discussed for more details.

Consider a cantilever beam as shown in Fig. 2. Boundary conditions for this beam contain two Dirichlet and two Neumann boundary conditions as follows:

$$U_1|_{\xi=0} = 0, \tag{14.1}$$

$$\Psi_1|_{\xi=0} = 0, \tag{14.2}$$

$$\Psi_n'|_{\xi=1} = 0, \tag{14.3}$$

$$(U_n' - \Psi_n)|_{\xi=1} = 0. \tag{14.4}$$

Starting with those at the left boundary condition and applying Eqs. (14.1) and (14.2) in Eqs. (9.1) and (9.2), results in the following expression:

$$\begin{Bmatrix} 0 \\ 0 \end{Bmatrix} = \begin{bmatrix} 1 & 0 & 1 & 0 \\ 0 & m_1 & 0 & -m_2 \end{bmatrix} \begin{Bmatrix} A_1 \\ B_1 \\ C_1 \\ D_1 \end{Bmatrix} = [\bar{\Lambda}]\{\mathrm{A}\}_{(1)}. \tag{15}$$

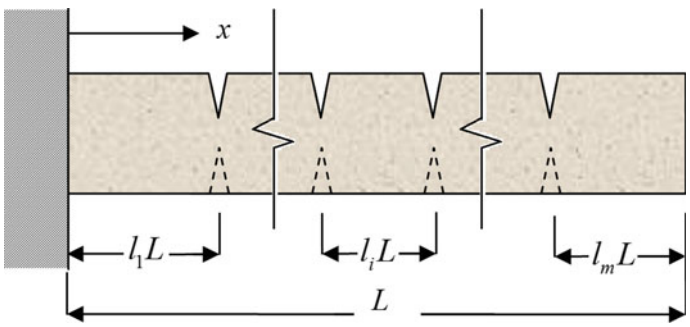

Fig. 2 Cantilever beam with arbitrary number of single- or double-sided open cracks

Satisfying the right boundary conditions by using Eqs. (14.3) and (14.4) in Eqs. (9.1) and (9.2) leads to a system of equations whose matrix form is

$$\begin{Bmatrix} 0 \\ 0 \end{Bmatrix} = \begin{bmatrix} m_1\beta_1 \cosh \beta_1 l_m & m_1\beta_1 \sinh \beta_1 l_m & m_2\beta_2 \cos \beta_2 l_m & m_2\beta_2 \sin \beta_2 l_m \\ (\beta_1 - m_1) \sinh \beta_1 l_m & (\beta_1 - m_1) \cosh \beta_1 l_m & -(\beta_2 + m_2) \sin \beta_2 l_m & (\beta_2 + m_2) \cos \beta_2 l_m \end{bmatrix} \begin{Bmatrix} A_m \\ B_m \\ C_m \\ D_m \end{Bmatrix} = [\Lambda]_{(m)} \ \{\mathrm{A}\}_{(m)}. \tag{16}$$

In general, this eigenvalue problem may be expressed as a fourth-order determinant for an arbitrary number of cracks. In each segment of the beam, the constant coefficients should be mapped into the constant ones of the first segment. This mapping process can be carried out using the following equations:

$$\{\mathrm{A}\}_{(n)} = \left[\prod_{i=1}^{n-1} [\mathrm{Z}]_{(i)}\right] \{\mathrm{A}\}_{(1)} \tag{17}$$

where

$$\left[\prod_{i=1}^{n-1} [\mathrm{Z}]_{(i)}\right] = [\mathrm{Z}]_{(1)}[\mathrm{Z}]_{(2)}[\mathrm{Z}]_{(3)} \cdots [\mathrm{Z}]_{(n-1)}. \tag{18}$$

In order to consider the right boundary conditions, the constants of the m-th segment of the beam should be mapped into the constants of the first segment using the below expressions:

$$\{\mathrm{A}\}_{(m)} = \left[\prod_{i=1}^{m-1} [\mathrm{Z}]_{(i)}\right] \{\mathrm{A}\}_{(1)}. \tag{19}$$

In general, the solution of the problem leads to a fourth-order determinant as follows:

$$\begin{Bmatrix} 0 \\ 0 \\ 0 \\ 0 \end{Bmatrix} = \begin{bmatrix} \bar{\Lambda}_{11} & \bar{\Lambda}_{12} & \bar{\Lambda}_{13} & \bar{\Lambda}_{14} \\ \bar{\Lambda}_{21} & \bar{\Lambda}_{22} & \bar{\Lambda}_{23} & \bar{\Lambda}_{24} \\ \Gamma_{11} & \Gamma_{12} & \Gamma_{13} & \Gamma_{14} \\ \Gamma_{21} & \Gamma_{22} & \Gamma_{23} & \Gamma_{24} \end{bmatrix} \begin{Bmatrix} A_1 \\ B_1 \\ C_1 \\ D_1 \end{Bmatrix} = \begin{bmatrix} [\bar{\Lambda}] \\ [\Gamma] \end{bmatrix} \begin{Bmatrix} A_1 \\ B_1 \\ C_1 \\ D_1 \end{Bmatrix} = [\Lambda_T]\{\mathrm{A}\}_{(1)}, \tag{20}$$

in which

$$[\Gamma] = [\Lambda]_{(m)} \left[\prod_{i=1}^{n} [\mathrm{Z}]_{(i)}\right]. \tag{21}$$

Therefore, in order to find non-trivial solutions of Eq. (20), the following condition should be satisfied:

$$\det [\Lambda_T] = 0. \tag{22}$$

Obviously, this approach can be used for a beam with arbitrary boundary conditions and arbitrary number of cracks. It should be noted that for other boundary conditions the solution may be reduced to a second-order determinant [14].

2.1 Cantilever beam with a crack

Expansion of Eq. (22) for a cantilever beam with a crack results in the following characteristic equation:

$$F_{ca}(m_1, m_2, \beta_1, \beta_2, l_1, l_2) \times \theta + G_{ca}(m_1, m_2, \beta_1, \beta_2) = 0, \tag{23.1}$$

in which

$$\begin{aligned}
&F_{ca}(m_1, m_2, \beta_1, \beta_2, l_1, l_2)\\
&= [m_2\beta_2(m_1 - \beta_1)\cosh l_2\beta_1 \sin l_2\beta_2 + m_1\beta_1(m_2 + \beta_2)\sinh l_2\beta_1 \cos l_2\beta_2]\\
&\quad \times \big[(m_1m_2^2\beta_2 + m_2m_1^2\beta_1 + m_1^2\beta_1\beta_2 - m_2^2\beta_1\beta_2)\cosh l_1\beta_1 \cos l_1\beta_2\\
&\quad - m_1m_2(m_2\beta_1 - m_1\beta_2 + 2\beta_1\beta_2)\sinh l_1\beta_1 \sin l_1\beta_2\\
&\quad - \ m_1m_2(\beta_2^2 - \beta_1^2 + m_1\beta_1 + m_2\beta_2)\big]\\
&\quad - [m_1\cosh l_1\beta_1 \sin l_1\beta_2 + m_2\sinh l_1\beta_1 \cos l_1\beta_2]\\
&\quad \times\big[2m_1m_2\beta_1\beta_2(m_2 + \beta_2)(m_1 - \beta_1)(1 - \cosh l_2\beta_1 \cos l_2\beta_2)\\
&\quad + \left(m_1^2\beta_1^2(m_2 + \beta_2)^2 - m_2^2\beta_2^2(m_1 - \beta_1)^2\right)\sinh l_2\beta_1 \sin l_2\beta_2\big]
\end{aligned} \tag{23.2}$$

and

$$\begin{aligned}
&G_{ca}(m_1, m_2, \beta_1, \beta_2)\\
&= (m_1\beta_2 + m_2\beta_1)\Big\{[m_2^2\beta_2(m_1 - \beta_1) + m_1^2\beta_1(m_2 + \beta_2)]\cos\beta_2\cosh\beta_1\\
&\quad + m_1m_2(m_2\beta_1 - m_1\beta_2 + 2\beta_1\beta_2)\sinh\beta_1\sin\beta_2\\
&\quad - m_1m_2\left(\beta_2^2 - \beta_1^2 + m_1\beta_1 + m_2\beta_2\right)\Big\}.
\end{aligned} \tag{23.3}$$

2.2 Cantilever beam with two cracks

For a cantilever beam with two cracks, the characteristic equation may be determined as a fourth-order determinant. The components of this determinant are illustrated in the Appendix. Using the computed determinant, natural frequencies of vibration may be determined. Finally, considering Eq. (20) and mapping matrices, mode shapes may be readily computed.

3 Forced response

Consider a multiple cracked beam under a unit moving load with a known constant velocity V. The load moves from the left end of the beam to the right end. The load position is obviously illustrated by Vt, in which t should be taken into account from the entrance of the moving load. In this research, the modal expansion method is employed to determine the forced response of the beam. The dynamic response of the cracked beam may be expressed as

$$y_f(x, t) = \sum_{i=1}^{N_m} q_i(t)Y_i(x), \tag{24.1}$$

$$\psi_f(x, t) = \sum_{i=1}^{N_m} q_i(t)\varphi_i(x), \tag{24.2}$$

in which $y_f(x, t)$ and $\psi_f(x, t)$ indicate the transverse deflection function and the slope of the deflection curve in the forced vibration, respectively. Furthermore, N_m is the total number of truncated terms; $q_i(t)$ denotes a generalized coordinate; $Y_i(x)$ and $\varphi_i(x)$ are piecewise continuous mode shapes calculated from the previous section. Based on Hamilton's principle for each mode, the equation of motion may be written as follows:

$$M_i^*\ddot{q}_i(t) + K_i^*q_i(t) = Q_i^*(t), \quad i = 1, 2, \ldots, N_m \tag{25}$$

where M_i^*, K_i^*, and $Q_i^*(t)$ are modal mass, modal stiffness, and modal loading in the i-th mode, respectively. Moreover, a super-dot denotes the differentiation with respect to time t.

The Lagrange equation of motion may be written as the well-known following form:

$$\frac{\partial}{\partial t}\left(\frac{\partial E_k}{\partial \dot{q}_i}\right) - \frac{\partial E_k}{\partial q_i} + \frac{\partial E_v}{\partial q_i} = Q_i, \tag{26}$$

in which E_k and E_v indicate the kinetic and potential energies, respectively. The kinetic energy of the beam may be written as below:

$$E_k = \frac{1}{2}\int_0^L m(x)\dot{y}^2(x,t)\mathrm{d}x + \frac{1}{2}\int_0^L I(x)\dot{\psi}^2(x,t)\mathrm{d}x. \tag{27}$$

It should be noted that rotational massless springs have no participation in the kinetic energy. Moreover, the potential energy is divided into two parts, $E_v = E_{vb} + E_{vc}$, in which E_{vb} and E_{vc} denote the potential energy in the beam and in the rotational springs, respectively. These two parts may be written as

$$E_{vb} = \frac{1}{2}\int_0^L k'(x)GA(x)[y'(x,t) - \psi(x,t)]^2\mathrm{d}x + \frac{1}{2}\int_0^L EI(x)\psi'^2(x,t)\mathrm{d}x \tag{28}$$

and

$$E_{vc} = \frac{1}{2}\sum_{i=1}^{m-1} K_{\mathrm{ci}}\left(\lim_{x\to L_i^+} y'(x,t) - \lim_{x\to L_i^-} y'(x,t)\right)^2, \tag{29}$$

where K_{ci} represents the stiffness of the i-th spring (corresponding to the i-th crack) and may be computed [25] as

$$K_{ci} = \frac{BH^2E}{72\pi\eta_i^2 f_J(\eta_i)}, \tag{30}$$

where $f_J(\eta_i)$ is known from Eq. (11.3) for a single-sided crack.

Using Eqs. (24.1) and (24.2), the kinetic and potential energies may be written as follows:

$$\begin{aligned} E_k = {} & \frac{1}{2}\sum_{i=1}^{N_m}\sum_{j=1}^{N_m}\left[\int_0^L m(x)Y_i(x)Y_j(x)\mathrm{d}x\right]\dot{q}_i(t)\dot{q}_j(t) \\ & + \frac{1}{2}\sum_{i=1}^{N_m}\sum_{j=1}^{N_m}\left[\int_0^L I(x)\varphi_i(x)\varphi_j(x)\mathrm{d}x\right]\dot{q}_i(t)\dot{q}_j(t) \end{aligned} \tag{31}$$

and

$$\begin{aligned} E_v = {} & \frac{1}{2}\sum_{i=1}^{N_m}\sum_{j=1}^{N_m}\left[\int_0^L k'(x)GA(x)[Y_i'(x) - \varphi_i(x)][Y_j'(x) - \varphi_j(x)]\mathrm{d}x\right]q_i(t)q_j(t) \\ & + \frac{1}{2}\sum_{i=1}^{N_m}\sum_{j=1}^{N_m}\left[\int_0^L EI(x)\varphi_i'(x)\varphi_j'(x)\mathrm{d}x\right]q_i(t)q_j(t) \\ & + \frac{1}{2}\sum_{i=1}^{N_m}\sum_{j=1}^{N_m}\sum_{k=1}^{m-1} K_{ck}\left(\lim_{x\to L_k^+} Y_i'(x) - \lim_{x\to L_k^-} Y_i'(x)\right)\left(\lim_{x\to L_k^+} Y_j'(x) - \lim_{x\to L_k^-} Y_j'(x)\right)q_i(t)q_j(t). \end{aligned} \tag{32}$$

Substituting Eqs. (31) and (32) into the Lagrange equation (26) and using modal orthogonality, the equations of motion for each mode may be available after some algebraic manipulations. Comparing the obtained equations of motion with Eq. (25), modal mass, modal stiffness, and generalized loading may be derived as

$$M_i^* = \rho A \int_0^L [Y_i^2(x) + r^2 \varphi_i^2(x)] \mathrm{d}x, \tag{33}$$

$$K_i^* = \int_0^L \left[E I \varphi_i'^2(x) + k' G A (Y_i'(x) - \varphi_i(x))^2 \right] \mathrm{d}x + \sum_{i=1}^{m-1} \frac{B H^2 E}{72 \pi \eta^2 f_J(\eta_i)} \left(\lim_{x \to L_i^+} Y_i'(x) - \lim_{x \to L_i^-} Y_i'(x) \right)^2, \tag{34}$$

$$Q_i^*(t) = \int_0^L Y_i(x) \delta(x - Vt) \mathrm{d}x = Y_i(Vt), \tag{35}$$

in which $\delta(.)$ denotes the Dirac delta function, and r is the radius of gyration of the beam cross-section. All other parameters have been described in previous Sections. After calculating these three parameters through Eqs. (33)–(35), the solution of the problem in each mode reduces to an ordinary second-order differential equation.

4 Numerical results and discussion

In order to verify the accuracy and efficiency of the proposed method, some parametric studies are presented in this Section. In the parametric studies, the effects of the crack parameters (i.e., location and depth), geometry of the beam, and the velocity of the moving load are presented. In the first step, a convergence test is carried out.

4.1 Convergence test and velocity effect

In the modal expansion method, the response of the structure may be represented by the sum of the determined responses in all modes. In continuous systems on the other hand, the number of modes is equal to infinity. From a practical viewpoint, the accurate response may be obtained from a limited number of the modes. In general, the sufficient number of modes depends on intrinsic characteristics of the structure, geometry, and loading content. In order to find the required sufficient number of modes in the proposed method, a convergence test is performed for a cantilever beam with a single-sided open crack. The geometric parameters used in this study are as follows: length-to-height ratios $\frac{L}{H} = 4$, 9, and 20, crack position ratio $e_1 = 0.5$, and crack depth ratio $\eta_1 = 0.5$. Moreover, the material parameters are as follows: Young's modulus $E = 210\,\mathrm{GPa}$, the shear modulus $G = 70\,\mathrm{GPa}$, and the material mass density $\rho = 7860\,\mathrm{Kg/m^3}$. To consider the load effect on the number of modes, three different load cases are taken into account. The velocity of the moving load for each geometry is 0.4, 0.8, and 1.2 times the critical velocity of the corresponding sound/uncracked Euler–Bernoulli beams ($V_{\mathrm{ce}} = \frac{1.8751}{L}\sqrt{\frac{EI}{\rho A}}$).

Figures 3, 4, 5 represent the results of this study for various length-to-height ratios and moving load velocities. In these figures, the horizontal axes represent the position of moving loads, whereas the vertical axes are the scaled deflections at the free end. The scaled deflections are derived by dividing the dynamic responses into the static ones at the free end due to a unit load at that point. In each study, the response is calculated by assuming 1, 2, 4, and 6 first modes. In the modal expansion method, the convergence rate mainly depends on the chosen test functions. Since in the present study test functions (mode shapes) are obtained analytically, the convergence rate is extremely rapid. As may be observed from these figures, participation of higher modes increases when length-to-height ratio decreases. In addition, a study for different moving load velocities indicates that when the velocity increases, the participation of higher modes increases. However, as a general result, considering of four first modes is definitely sufficient for a practical problem.

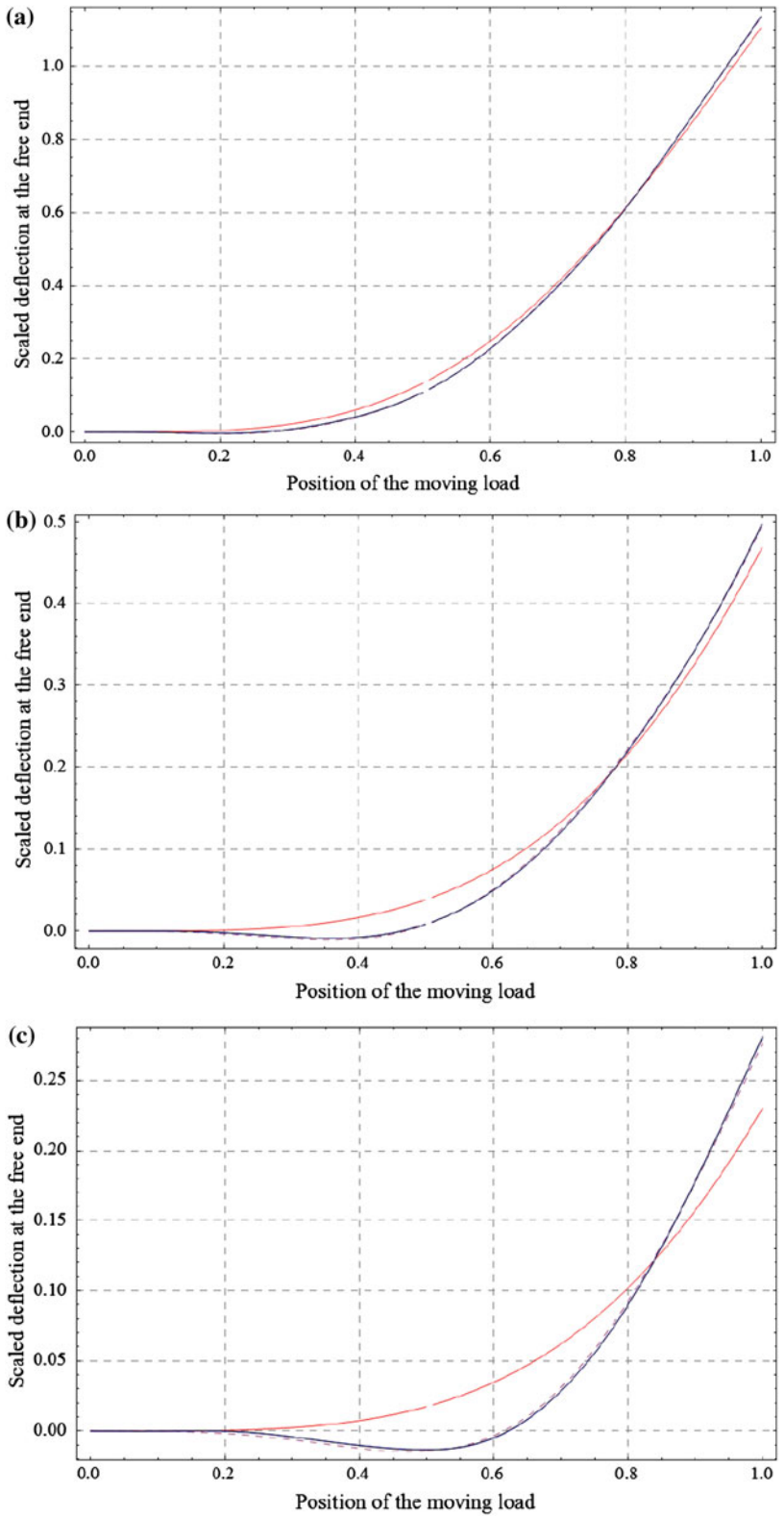

Fig. 3 Scaled deflection at the free end of a cantilever beam with $\frac{L}{H} = 20$, subject to a moving load, calculated assuming 1, 2, 4, and 6 modes (indicated by *red, dashed, blue, and black lines*, respectively); **a** moving load velocity $= 0.4V_{ce}$, **b** moving load velocity $= 0.8V_{ce}$, **c** moving load velocity $= 1.2V_{ce}$

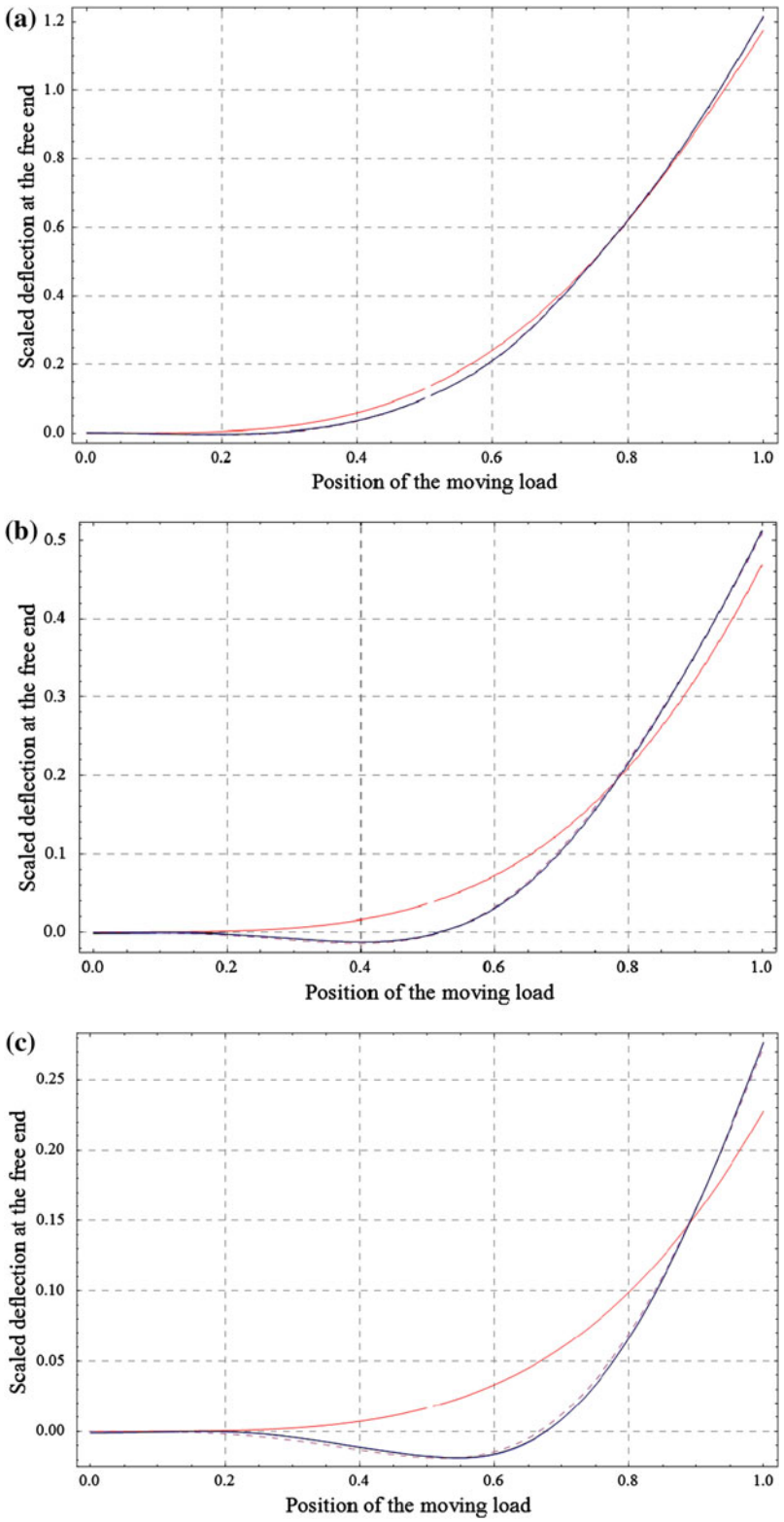

Fig. 4 Scaled deflection at the free end of a cantilever beam with $\frac{L}{H} = 9$, subject to a moving load, calculated assuming 1, 2, 4, and 6 modes (indicated by *red, dashed, blue, and black lines*, respectively); **a** moving load velocity $= 0.4V_{ce}$, **b** moving load velocity $= 0.8V_{ce}$, **c** moving load velocity $= 1.2V_{ce}$

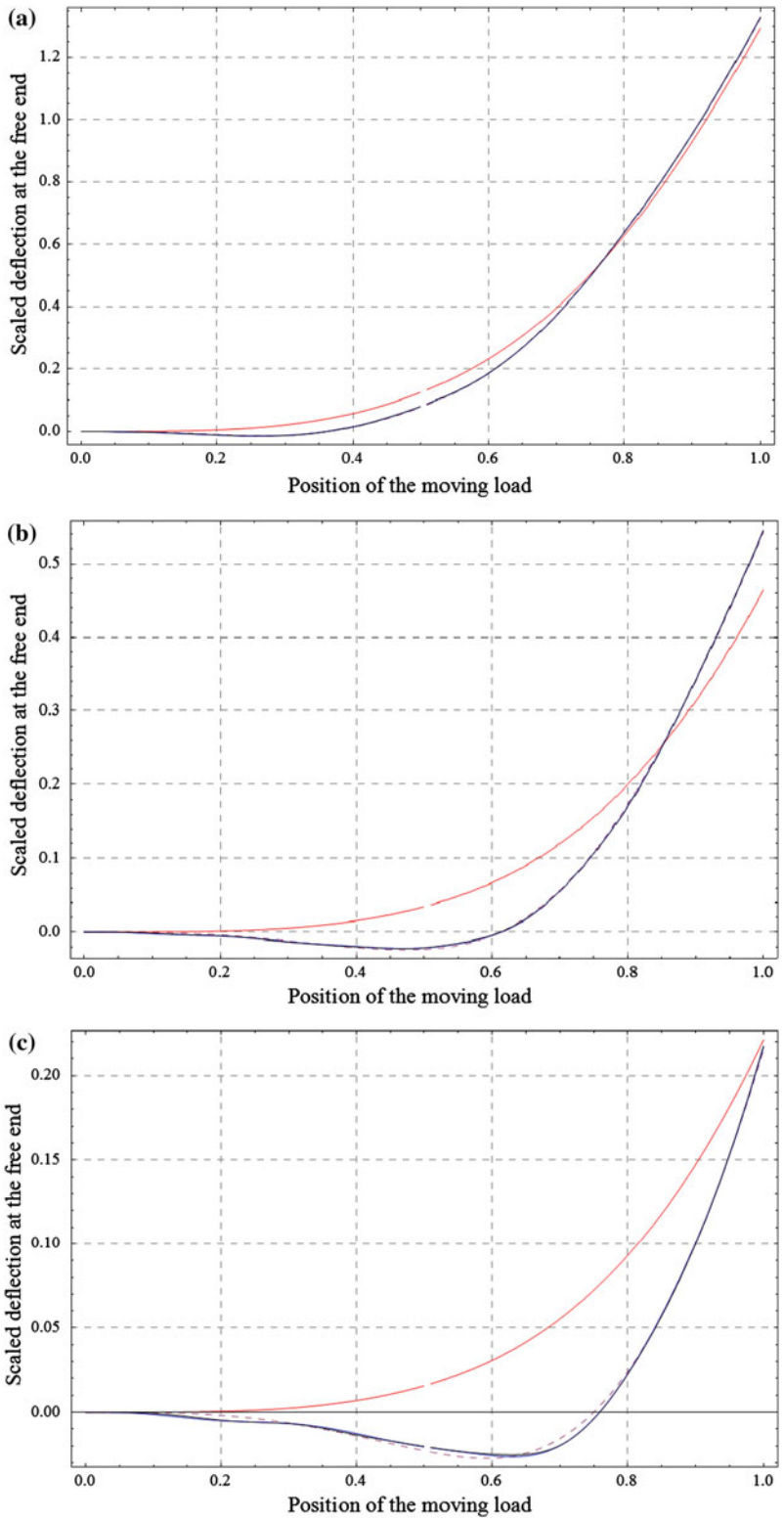

Fig. 5 Scaled deflection at the free end of a cantilever beam with $\frac{L}{H} = 4$, subject to a moving load, calculated assuming 1, 2, 4, and 6 modes (indicated by *red, dashed, blue, and black lines*, respectively); **a** moving load velocity $= 0.4V_{ce}$, **b** moving load velocity $= 0.8V_{ce}$, **c** moving load velocity $= 1.2V_{ce}$

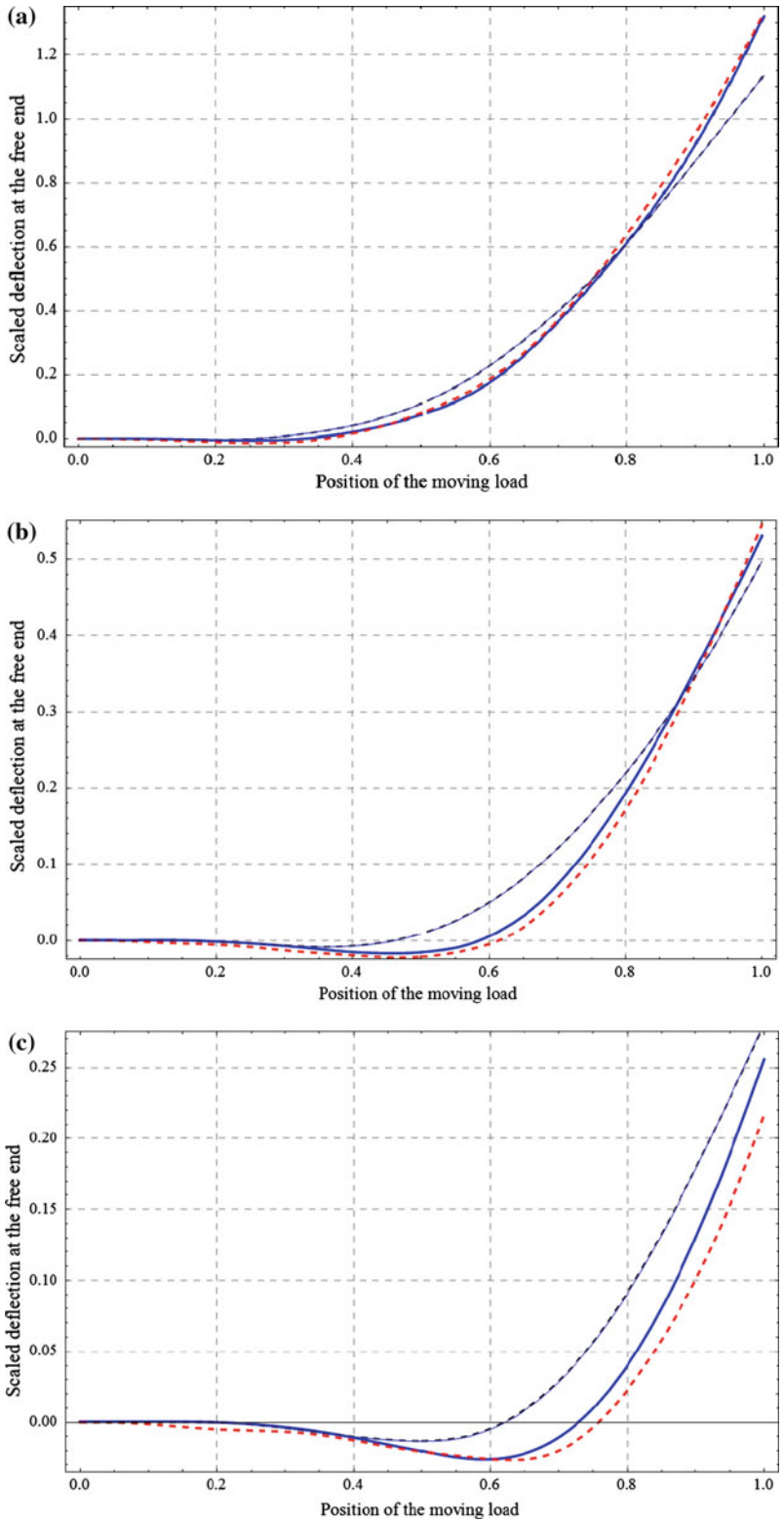

Fig. 6 Scaled deflection at the free end of a cantilever beam for Euler–Bernoulli and Timoshenko beam models, for Euler–Bernoulli model with $\frac{L}{H} = 4$, Timoshenko model with $\frac{L}{H} = 4$, Euler–Bernoulli model with $\frac{L}{H} = 20$, and Timoshenko model with $\frac{L}{H} = 20$ (indicated by *thick blue, dashed red, thin blue, and dashed black lines*, respectively); **a** moving load velocity $= 0.4V_{ce}$, **b** moving load velocity $= 0.8V_{ce}$, **c** moving load velocity $= 1.2V_{ce}$

Furthermore, the figures indicate that for different moving load velocities, when the velocity of the moving load increases, the response of the system decreases in the presence of the moving load. In all presented cases of this research, maximum response of the beam occurs after the time at which the moving load leaves the beam.

4.2 Effects of shear deformations and rotational inertia

In order to study the effects of rotational inertia and shear deformations, Euler–Bernoulli and Timoshenko beam models are considered for the same problems. In these problems, a cantilever beam with a single-sided open crack with crack depth ratio $\eta_1 = 0.5$, and different length-to-height ratios ($\frac{L}{H} = 4, 20$) are investigated. For all cases, the crack is assumed to be located at the mid-span of the beam ($e_1 = 0.5$). The moving load velocity for each geometry is 0.4, 0.8, and 1.2 times that of V_{ce}. For each model, free and forced responses of the corresponding Euler–Bernoulli beam are computed using the method proposed in [19]. Results of the analyses are shown in Fig. 6. A comparison of the beams' responses in these models shows that in the beams with $\frac{L}{H} = 20$ these two models lead to relatively similar results. In beams with $\frac{L}{H} = 4$, different behaviors are obtained when the velocity of the moving load changes. For the case of $0.4V_{ce}$, the two models again result in the same responses; whereas, when the velocity of the moving load increases, the difference of responses in these two models increases. As may be observed from Fig. 6c, the tip deflection is larger for the case of an Euler–Bernoulli beam in comparison with a Timoshenko beam. This fact may arise from the effect of rotational inertia. For this example, as the loading time is very short so that the moving load leaves the beam rapidly, the inertia effect is clearer than shear deformations. Obviously, the effects of rotational inertia and shear deflections may be predicted according to the geometry, loading, and intrinsic characteristics of the structure.

4.3 Effect of crack depth

A cantilever beam with a single-sided open crack with different non-dimensional crack depth ratios ($\eta_1 = 0.2$, 0.35, 0.5, and 0.7) and different length-to-height ratios ($\frac{L}{H} = 4$, 9, and 20) is investigated in this Section. For all cases, the crack is assumed to be located at the mid-span of the beam ($e_1 = 0.5$). When the crack depth

Table 1 Circular natural frequencies for different crack depth ratios (η_1) and various length-to-height ratios (L/H)

	Circular natural frequencies											
	$L/H = 4$				$L/H = 9$				$L/H = 20$			
η_1	f_1	f_2	f_3	f_4	f_1	f_2	f_3	f_4	f_1	f_2	f_3	f_4
0	1244.95	6184.58	14020.7	22397.9	576.64	3402.8	8787.41	15644.1	261.74	1619	4442.58	8466.8
0.20	1218.06	5779.12	13942.8	21729.9	570.7	3268.26	8783.3	15200.1	260.5	1586.8	4442.4	8317.46
0.35	1161.55	5152.83	13827.4	20822.9	557.66	3025.04	8775.9	14499.3	257.72	1521.5	4442	8039.8
0.50	1067.37	4495.82	13713.4	20048.3	534.02	2706.1	8766.5	13756.4	252.45	1418.5	4441.4	7664.5
0.70	906.47	3878.07	13613.5	19467.7	486.77	2316.4	8755.2	13063.1	240.9	1256.2	4440.5	7198.1

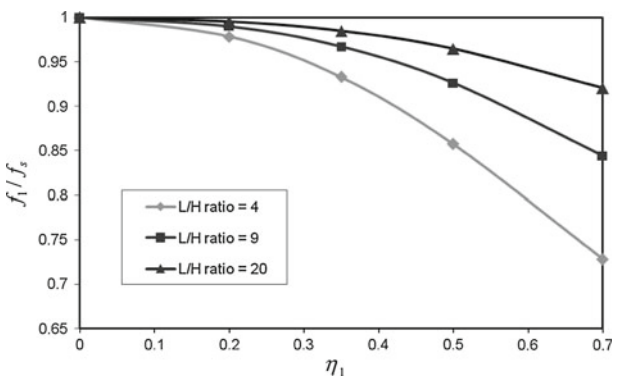

Fig. 7 The variation of fundamental frequencies of the cantilever beam for various crack depth ratios

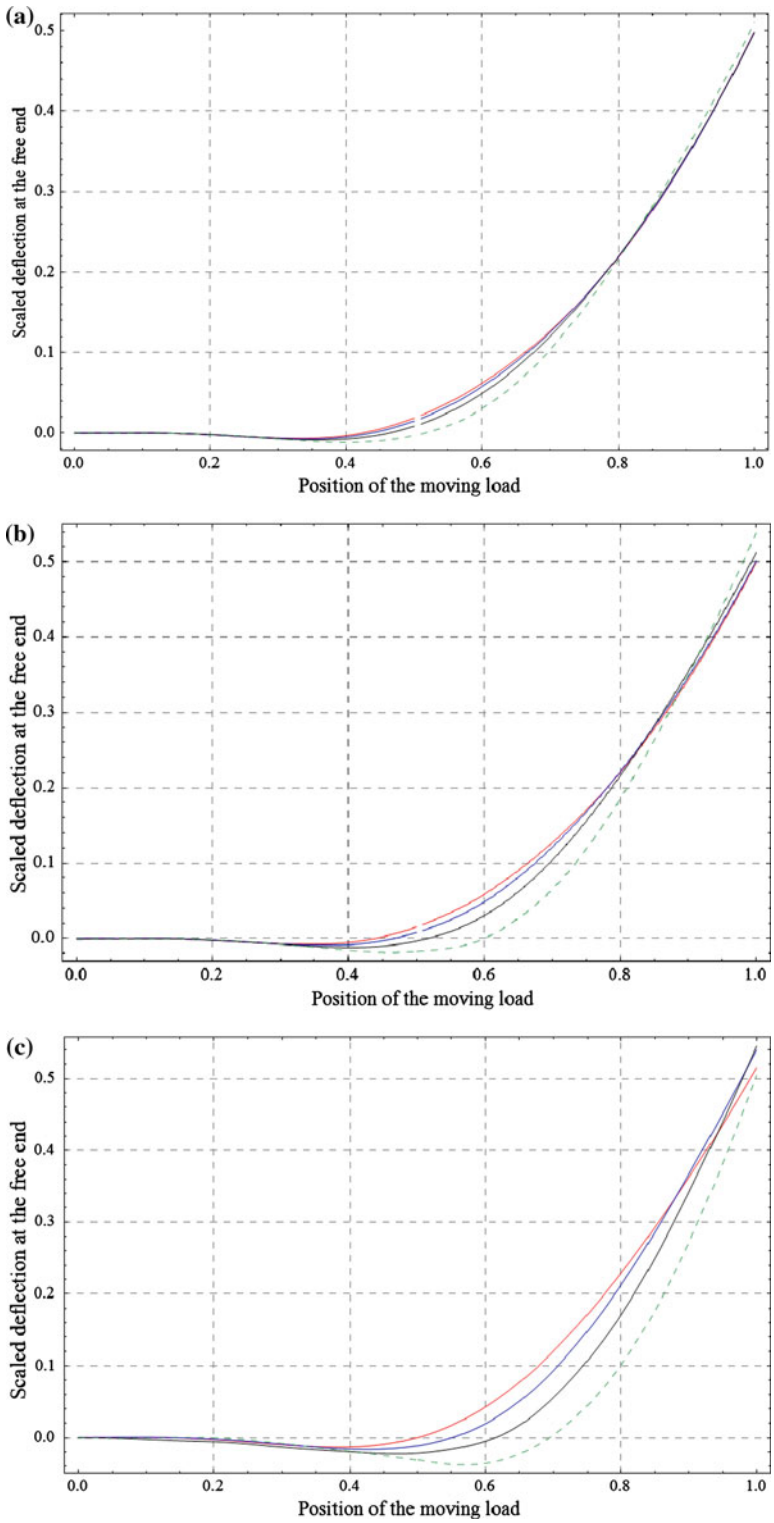

Fig. 8 Scaled deflection at the free end of a cantilever beam with $e_1 = 0.5$, subject to a moving load velocity of $0.8V_{ce}$, for different crack depth ratios η_1 =0.2, 0.35, 0.5, and 0.7 (indicated by *red, blue, black, and dashed lines*, respectively); **a** $\frac{L}{H} = 20$, **b** $\frac{L}{H} = 9$, **c** $\frac{L}{H} = 4$

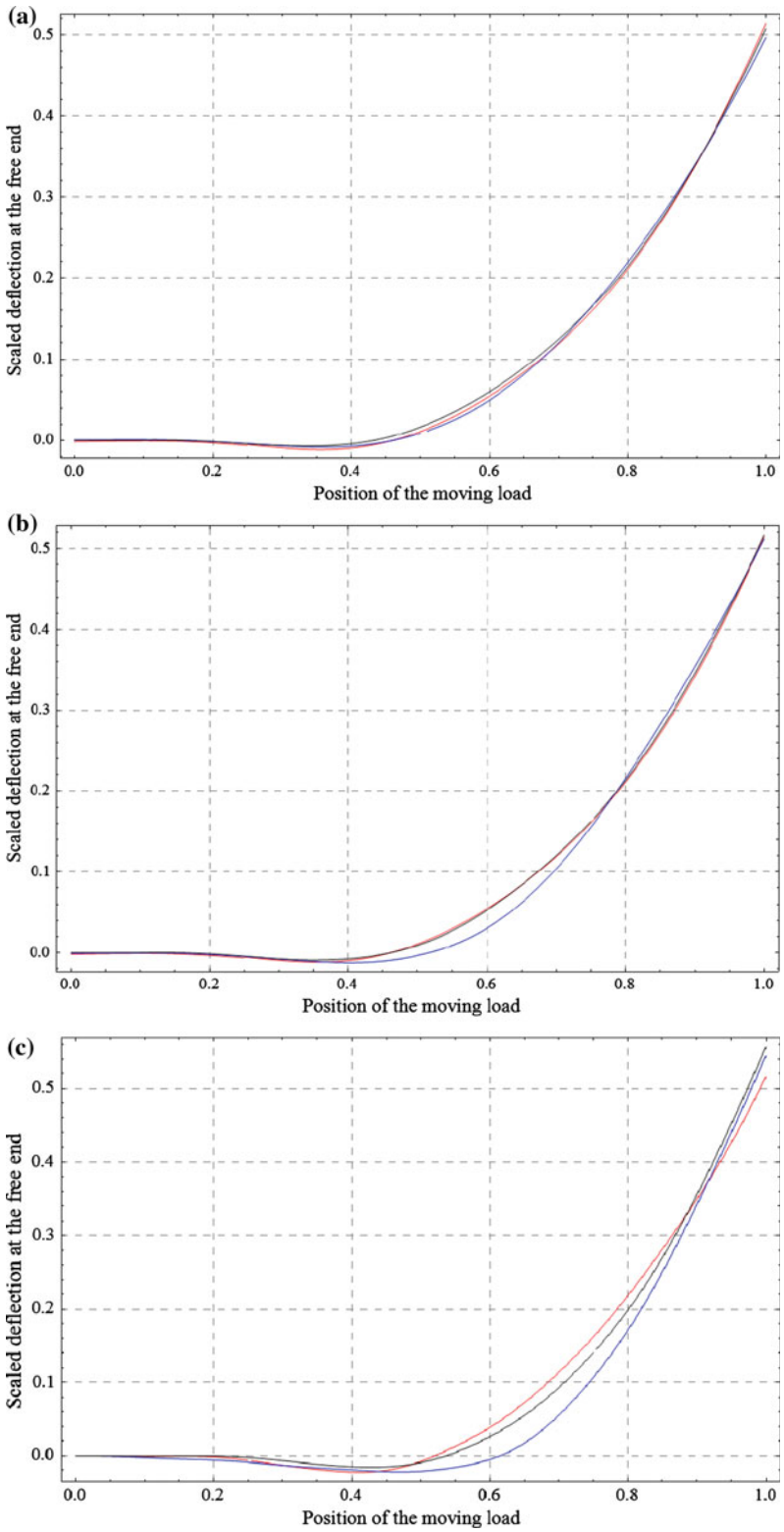

Fig. 9 Scaled deflection at the free end of a cantilever beam with $\eta_1 = 0.5$, subject to a moving load velocity of $0.8V_{\text{ce}}$, for various crack location ratios e_1 =0.25, 0.5, and 0.75 (indicated by *red, blue, and black lines*, respectively); **a** $\frac{L}{H} = 20$, **b** $\frac{L}{H} = 9$ **c** $\frac{L}{H} = 4$

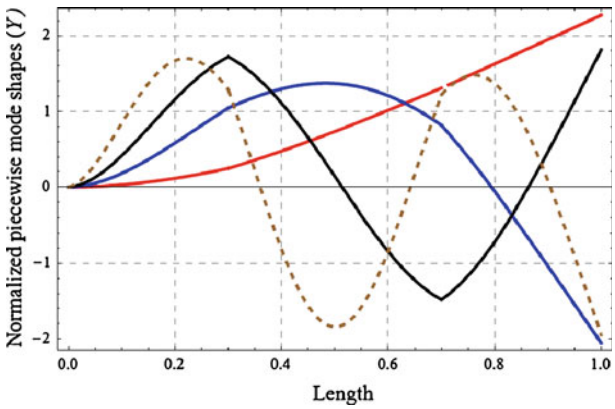

Fig. 10 Normalized piecewise mode shapes for the first four modes of vibration of a cantilever beam with two single-sided edge cracks

increases, the stiffness and natural frequencies of the beam decrease. Variations of the natural frequencies for deep beams are relatively more pronounced than for shallow beams (see Table 1). Figure 7 shows the variation of fundamental frequencies of the beam for different crack depths. In this figure, the horizontal axis indicates the non-dimensional crack depth ratio (η_1), whereas the vertical axis represents the fundamental frequencies of the cracked beam divided by the fundamental frequency of the sound beam (f_1/f_s). In order to study the effects of the crack depth on a moving load, we assume the moving load velocity for each geometry to be 0.8 times that of the critical velocity of the corresponding sound Euler–Bernoulli beam. Figure 8 illustrates the results of the scaled deflection at the free end of the beam for various crack depth ratios. In general, the results show that the response of the beam is not sensitive to the crack depth ratios, especially for practical length-to-height ratios.

4.4 Effect of crack location

In this Section, cantilever Timoshenko beams with different non-dimensional crack location ratios ($e_1 = 0.25$, 0.5, and 0.75) are investigated. For all cases, the crack depth ratio is assumed $\eta_1 = 0.5$. As in the previous Section, various length-to-height ratios ($\frac{L}{H} = 4$, 9, and 20) are examined. Furthermore, the velocity of the moving load for each geometry is assumed to be 0.8 times that of V_{ce}. The results are plotted in Fig. 9.

4.5 Beam with arbitrary number of cracks

Consider a cantilever beam with two single-sided edge cracks. The geometry parameters used in this study are as follows: $\frac{L}{H} = 20$, crack position ratios $e_1 = 0.3$ and $e_2 = 0.7$, crack depth ratios $\eta_1 = \eta_2 = 0.5$, and the

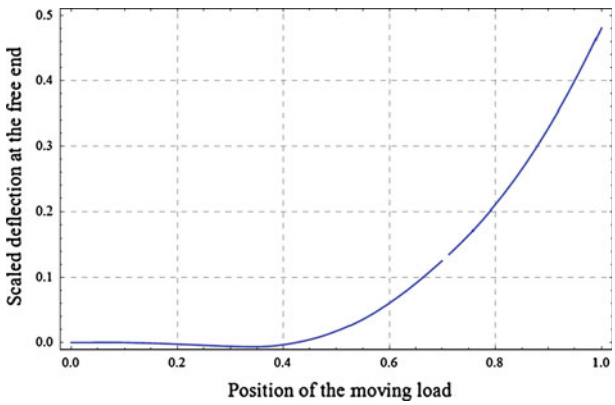

Fig. 11 Scaled deflection at the free end of a cantilever beam with two single-sided edge cracks

velocity of the moving load $= 0.8V_{ce}$. The normalized mode shapes of the beam are evaluated and presented in Fig. 10. Moreover, the response of the beam under the moving load is also determined (see Fig. 11).

5 Conclusions

Free and forced vibrations of Timoshenko beam with an arbitrary number of cracks subjected to a concentrated moving load were analytically investigated in this paper. The modal expansion method was employed to determine the forced vibration response. The convergence test was carried out for various length-to-height ratios and moving load velocities. The obtained results indicated that the convergence rate is extremely rapid in the proposed analytical solution. For higher moving load velocities and lower length-to-height ratios of the beam, participation of the higher modes increases. For various crack depth ratios, the results showed that the response of the beam is not so sensitive to the crack depth.

Appendix

As discussed in Sect. 2.2, the characteristic equation for the free vibration of a beam with an arbitrary number of cracks and arbitrary boundary conditions can be written as a fourth-order determinant of $[R]$ matrix. As a sample, the $R\{i, j\}$ components of $[R]$ matrix $(i, j = 1, \ldots, 4)$ for a cantilever beam with two cracks are as follows:

$$R\{1,1\} = Sh(\beta_1)(\beta_1 - m_1) + \theta_2 \frac{Ch(l_3'\beta_1)}{m_2\beta_1 + m_1\beta_2} F_4 + \theta_1 \frac{Ch(l_1\beta_1)}{(m_2\beta_1 + m_1\beta_2)^2}(F_2F_4\theta_2 + F_5), \tag{A.1}$$

$$R\{1,2\} = Ch(\beta_1)(\beta_1 - m_1) + \theta_2 \frac{Sh(l_3'\beta_1)}{m_2\beta_1 + m_1\beta_2} F_4 + \theta_1 \frac{Sh(l_1\beta_1)}{(m_2\beta_1 + m_1\beta_2)^2}(F_2F_4\theta_2 + F_5), \tag{A.2}$$

$$R\{1,3\} = -S(\beta_2)(\beta_2 + m_2) + \theta_2 \frac{m_2\beta_2 C(l_3'\beta_2)}{m_1\beta_1(m_2\beta_1 + m_1\beta_2)} F_4 + \theta_1 \frac{m_2\beta_2 C(l_1\beta_2)}{m_1\beta_1(m_2\beta_1 + m_1\beta_2)^2}(F_2F_4\theta_2 + F_5), \tag{A.3}$$

$$R\{1,4\} = C(\beta_2)(\beta_2 + m_2) + \theta_2 \frac{m_2\beta_2 S(l_3'\beta_2)}{m_1\beta_1(m_2\beta_1 + m_1\beta_2)} F_4 + \theta_1 \frac{m_2\beta_2 S(l_1\beta_2)}{m_1\beta_1(m_2\beta_1 + m_1\beta_2)^2}(F_2F_4\theta_2 + F_5), \tag{A.4}$$

$$R\{2,1\} = m_1\beta_1 Ch(\beta_1) + \theta_2 \frac{Ch(l_3'\beta_1)F_1}{m_2\beta_1 + m_1\beta_2} + \theta_1 \frac{Ch(l_1\beta_1)}{(m_2\beta_1 + m_1\beta_2)^2}(F_1F_2\theta_2 + F_3), \tag{A.5}$$

$$R\{2,2\} = m_1\beta_1 Sh(\beta_1) + \theta_2 \frac{Sh(l_3'\beta_1)F_1}{m_2\beta_1 + m_1\beta_2} + \theta_1 \frac{Sh(l_1\beta_1)}{(m_2\beta_1 + m_1\beta_2)^2}(F_1F_2\theta_2 + F_3), \tag{A.6}$$

$$R\{2,3\} = m_2\beta_2 C(\beta_2) + \theta_2 \frac{C(l_3'\beta_1)F_1}{m_2\beta_1 + m_1\beta_2} + \theta_1 \frac{C(l_1\beta_2)}{(m_2\beta_1 + m_1\beta_2)^2}(F_1F_2\theta_2 + F_3), \tag{A.7}$$

$$R\{2,4\} = m_2\beta_2 S(\beta_2) + \theta_2 \frac{S(l_3'\beta_1)F_1}{m_2\beta_1 + m_1\beta_2} + \theta_1 \frac{S(l_1\beta_2)}{(m_2\beta_1 + m_1\beta_2)^2}(F_1F_2\theta_2 + F_3), \tag{A.8}$$

$$\begin{aligned} &R\{3,1\} = 1, \quad R\{3,2\} = 0, \quad R\{3,3\} = 1, \quad R\{3,4\} = 0, \\ &R\{4,1\} = 0, \quad R\{4,2\} = m_1, \quad R\{4,3\} = 1, \quad R\{4,4\} = -m_2 \end{aligned} \tag{A.9}$$

where *S, Sh, C* and *Ch* denote Sin, Sinh, Cos and Cosh functions, respectively. In addition, $l_1' = l_2 + l_3$, $l_2' = l_3 + l_1$, $l_3' = l_1 + l_2$, and

$$F_1 = m_2\beta_2(m_1 - \beta_1)S(l_3\beta_2) + m_1\beta_1(m_2 + \beta_2)Sh(l_3\beta_1), \tag{A.10}$$

$$F_2 = m_2\beta_2(m_1 - \beta_1)S(l_2\beta_2) + m_1\beta_1(m_2 + \beta_2)Sh(l_2\beta_1), \tag{A.11}$$

$$F_3 = (m_2\beta_1 + m_1\beta_2)(m_1\beta_1(m_2 + \beta_2)Sh(l_1'\beta_1) + m_2\beta_2(m_1 - \beta_1)S(l_1'\beta_2)), \tag{A.12}$$

$$F_4 = m_1\beta_1(m_1 - \beta_1)(m_2 + \beta_2)(C(l_3\beta_2) - Ch(l_3\beta_1)), \tag{A.13}$$

$$F_5 = m_1\beta_1(m_2\beta_1 + m_1\beta_2)(m_1 - \beta_1)(m_2 + \beta_2)(C(l_1'\beta_2) - Ch(l_1'\beta_1)). \tag{A.14}$$

References

1. Kienzler, R., Herrmann, G.: An elementary theory of defective beams. Acta Mech. **62**, 37–46 (1986)
2. Doebling, S.W., Farrar, C.R., Prime, M.B., Shevitz, D.W.: Damage Identification and Health Monitoring of Structural and Mechanical Systems from Changes in Their Vibration Characteristics: a literature review. Los Alamos National Laboratory, LA-13070-MS (1996)
3. Chondros, T.G., Dimarogonas, A.D.: Influence of a crack on the dynamic characteristics of structures. J. Vib. Acoust. Stress Reliab. Des. **111**, 251–256 (1989)
4. Adams, R.D., Cawley, P., Pye, C.J., Stone, B.J.: A vibration technique for non-destructively assessing the integrity of structures. J. Mech. Eng. Sci. **20**, 93–100 (1978)
5. Rizos, P.F., Aspragathos, N., Dimarogonas, A.D.: Identification of crack location and magnitude in a cantilever beam from the vibration modes. J. Sound Vib. **138**, 381–388 (1990)
6. Liang, R.Y., Hu, J., Choy, F.: Theoretical study of crack-induced eigenfrequency changes on beam structures. ASCE J. Eng. Mech. **118**, 384–396 (1992)
7. Krawczuk, M.: Natural vibration of cracked rotating beams. Acta Mech. **99**, 35–48 (1993)
8. Chondros, T.G., Dimarogonas, A.D., Yao, J.: A continuous cracked beam vibration theory. J. Sound Vib. **215**, 17–34 (1998)
9. Chinchalkar, S.: Detection of the crack location in beams using natural frequencies. J. Sound Vib. **247**, 417–429 (2001)
10. Saavedra, P.N., Cuitino, L.A.: Crack detection and vibration behavior of cracked beams. Comput. Struct. **79**, 1451–1459 (2001)
11. Nahvi, H., Jabbari, M.: Crack detection in beams using experimental modal data and finite element model. Int. J. Mech. Sci. **47**, 1477–1497 (2005)
12. Lele, S.P., Maiti, S.K.: Modeling of transverse vibration of short beams for crack detection and measurement of crack extension. J. Sound Vib. **257**, 559–583 (2002)
13. Lin, H.-P.: Direct and inverse methods on free vibration analysis of simply supported beams with a crack. Eng. Struct. **26**, 427–436 (2004)
14. Khaji, N., Shafiei, M., Jalalpour, M.: Closed-form solutions for crack detection problem of Timoshenko beams with various boundary conditions. Int. J. Mech. Sci. **51**, 667–681 (2009)
15. Jaiswal, O.R., Iyengar, R.N.: Dynamic response of a beam on elastic foundation of finite depth under a moving force. Acta Mech. **96**, 67–83 (1993)
16. Hasheminejad, S.M., Rafsanjani, A.: Two-dimensional elasticity solution for transient response of simply supported beams under moving loads. Acta Mech. **217**, 205–218 (2011). doi:10.1007/s00707-010-0393-7
17. Lee, H.P., Ng, T.Y.: Dynamic response of a cracked beam subject to a moving load. Acta Mech. **106**, 221–230 (1994)
18. Mahmoud, M.A.: Stress intensity factors for single and double edge cracks in a simple beam subject to a moving load. Int. J. Fract. **111**, 151–161 (2001)
19. Lin, H.P., Chang, S.C.: Forced responses of cracked cantilever beams subjected to a concentrated moving load. Int. J. Mech. Sci. **48**, 1456–1463 (2006)
20. Yang, J., Chen, Y., Xiang, Y., Jia, X.L.: Free and forced vibration of cracked inhomogeneous beams under an axial force and a moving load. J. Sound Vib. **312**, 166–181 (2008)
21. Timoshenko, S., Young, D.H., Weaver, W.: Vibration Problems in Engineering. Wiley, New York (1974)
22. Huang, T.: The effect of rotary inertia and of shear deformation on the frequency and normal mode equations of uniform beams with simple end conditions. ASCE J. Appl. Mech. **53**, 579–584 (1961)
23. Haisty, B.S., Springer, W.T.: A general beam element for use in damage assessment of complex structures. J. Vib. Acoust. Stress Reliab. Des. **110**, 389–394 (1988)
24. Ostachowitz, W.M., Krawczuk, M.: Analysis of the effect of cracks on the natural frequencies of a cantilever beam. J. Sound Vib. **150**, 191–201 (1991)
25. Atluri, S.N.: Computational Methods in the Mechanics of Fracture. North-Holland, Amsterdam (1986)